EXIT Analysis for 5G NR QC-LDPC Codes Based on Base Graphs 1 and 2

Yoga Julian, Rina Pudji Astuti, and Khoirul Anwar
Center for Advanced Wireless Technologies (AdWiTech), School of Electrical Engineering,
Telkom University, Jl. Telkomunikasi No. 1, Terusan Buah Batu, Bandung, 40257 INDONESIA
Email: {yogajuliantt@student., rinapudjiastuti@, anwarkhoirul@}telkomuniversity.ac.id.

***Abstract*—Quasi-Cyclic (QC) Low Density Parity Check (LDPC) codes constructed based on Base Graphs (BG) 1 and 2 have been standardized as channel coding schemes for the fifth telecommunication generation (5G) New Radio (NR). This paper analyses the behaviour of QC-LDPC codes of 5G NR based on BG-1 and BG-2 to evaluate BG selection for practical applications. In this paper, we consider a single carrier transmission under additive white Gaussian noise (AWGN) channels. We use Extrinsic Information Transfer (EXIT) chart to evaluate and predict the performances as well as the behaviour of the QC-LDPC codes based on BG-1 and BG-2.**

***Index Terms*—QC-LDPC codes, EXIT Analysis, Channel coding, 5G NR.**

I. Introduction

QC-LDPC codes in 5G NR are in principle based on Protograph Based Raptor-like (PBRL) [1]. The QC-LDPC codes have good performances on wide range of block-length and coding rate R to meet optimal transmission below the channel capacity $\mathcal{C}$ [2].

5G NR requires Rate Compatible (RC) codes to support Incremental Redundancy (IR) Hybrid Automatic Repeat Request (HARQ) systems. Puntured Information are carefully designed to ensure good error performance across the family of 5G NR code rates [3]. On the other hands, lifting process of 5G NR QC-LDPC codes follows Circulant Progressive Edge Growth (CPEG) constraint to avoid short cycles and stopping sets. In this paper, we extend our work in [4] for BG-2 to complete the analysis.

II. System Model

We consider a system model folowing [4] to evaluate the 5G NR QC-LDPC codes with parity check matrix $\mathbf{H}$ from [5]. We consider a single user scheme communicating to/from base station.

III. EXIT Chart of 5G NR QC-LDPC Codes

Since EXIT chart is drawn between variable nodes (VND) V and check nodes (CND) C, the involved mutual informations (MI) are $I^{int}_{A,C}, I^{int}_{E,C}, I^{int}_{A,V}, I^{int}_{E,V}$ expressing the *a priori* MI of CND, the extrinsic MI from CND, the *a priori* MI of VND, and extrinsic MI from VND, respectively. When Extended Parity (EP) is taken into account, MI involving extended variable node (EVND) $\tilde{V}$ and extended check node (ECND) $\tilde{C}$ should be taken into account with $I^{int}_{A,\tilde{C}}, I^{int}_{E,\tilde{C}}, I^{int}_{A,\tilde{V}}, I^{int}_{E,\tilde{V}}$ expressing the *a priori* MI of ECND, the extrinsic MI from ECND, the *a priori* MI of EVND, and extrinsic MI from EVND, respectively. On the other hand the information exchange from LDPC codes to/from EP and vice versa is denoted by $I^{ext}_{A,V}$ $I^{ext}_{E,V}, I^{ext}_{A,\tilde{V}}$ $I^{ext}_{E,\tilde{C}}$ expressing the external *a priori* MI of VND, the external extrinsic MI from VND, the external *a priori* MI of EVND, and external extrinsic MI from EVND, respectively.

To simplify the analysis, we measure MI using J-function $J(\cdot)$ and its inverse $J^{-1}(\cdot)$, of which the details are presented in [6]. The relationship between variance and MI is

$$\sigma = J^{-1}(I_A), \tag{1}$$

where $\sigma^2 = \frac{4}{\sigma_n^2}$ with on being the noise variance. The EXIT chart of BG-1 is shown in Fig. 2 drawn based on MI between

$$I^{int}_{E,V} = \sum_i \mathcal{F}^{\Lambda}_i J\left(\sqrt{(d_{V_i}-1)[J^{-1}(I^{int}_{A,V})]^2 + [J^{-1}(I^{ext}_{A,V})]^2}\right), \tag{2}$$

where $\mathcal{F}^{\Lambda}_i$ is the i-th fraction of $\Lambda_{LDPC}(x)$ and

$$I^{int}_{E,C} = 1 - \sum_i \mathcal{F}^{\Omega}_i J\left(\sqrt{(d_{C_i}-1)[J^{-1}(1 - I^{int}_{A,C})]^2}\right), \tag{3}$$

where $\mathcal{F}^{\Omega}_i$ is the i-th fraction of $\Omega_{LDPC}(x)$ and $I^{ext}_{A,V}$ is *a priori* MI from the external iteration. d_V and d_C are the degree of VND and CND respectively. $I^{ext}_{A,V}$ is depending on

$$I^{ext}_{E,\tilde{V}} = \sum_i \mathcal{F}^{\Lambda}_{i,EP} J\left(\sqrt{(d_{\tilde{V}_i})[J^{-1}(I^{int}_{A,\tilde{V}})]^2 + [J^{-1}(I_{A_{ch}})]^2}\right) \tag{4}$$

with $\mathcal{F}^{\Lambda}_{i,EP}$ being the i-th fraction of $\Lambda_{EP}(x)$ and $d_{\tilde{V}_i}$ being the degree of the i-th EP VND. It can be observed from (4) that in the case of EP is not transmitted, then $I^{int}_{A,\tilde{V}} = 0$ resulting $I^{ext}_{E,\tilde{V}} = I_{A_{ch}} = I^{ext}_{A,V}$. The value of $I^{int}_{A,\tilde{V}}$ depends on

$$I^{int}_{E,\tilde{C}} = 1 - \sum_i \mathcal{F}^{\Omega}_{i,EP} J\Big[d_{\tilde{C}_i} - 1)[J^{-1}(1 - I^{int}_{A,\tilde{C}})]^2 + [J^{-1}(1 - I_{A_{ch}})]^2\Big]^{\frac{1}{2}}, \tag{5}$$

This research is in part supported by the Telkom University Scientific Research Grant of "Hibah Penelitian Internasional 2018" on Polar-Raptor Codes-Structured Super-Dense Networks for The Internet-of-Things (IoT) and Insinas 5G-POINT, 2018–2019.

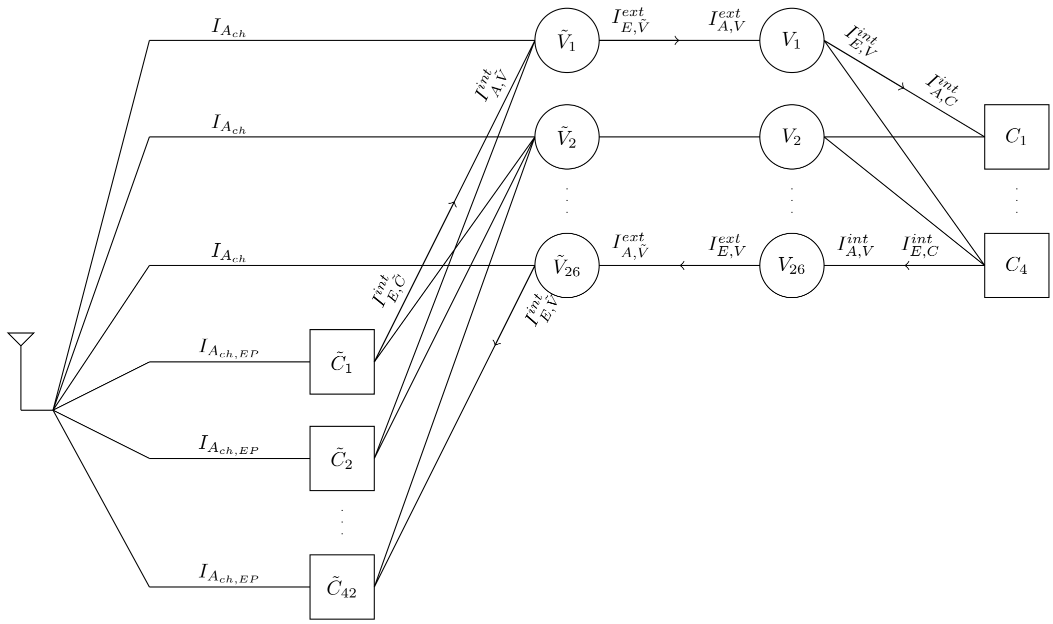

Fig. 1: Bipartite graph of 5G NR QC-LDPC codes based on BG-1 showing extended parity with $\tilde{V}$ and $\tilde{C}$.

where $\mathcal{F}^{\Omega}_{i,EP}$ is the i-th fraction of $\Omega_{EP}(x)$ and $I^{int}_{A,\tilde{C}}$ is obtained from

$$I^{int}_{E,\tilde{V}} = \sum_i \mathcal{F}^{\Lambda}_{i,EP} J \Big[(d_{\tilde{V}_i} - 1)[J^{-1}(I^{int}_{A,\tilde{V}})]^2 + [J^{-1}(I^{ext}_{A,\tilde{V}})]^2 + \sigma^2_{ch} \Big]^{\frac{1}{2}}, \quad (6)$$

where the value of $I^{ext}_{A,\tilde{V}}$ is determined by

$$I^{ext}_{E,V} = \sum_i \mathcal{F}^{\Lambda}_i J \left(\sqrt{(d_{V_i})[J^{-1}(I^{int}_{A,C})]^2 + [J^{-1}(I^{ext}_{A,V})]^2} \right). \quad (7)$$

All the MI used in (2-7) are based on

$$\Lambda_{LDPC1}(x) = \frac{3}{26}x^2 + \frac{22}{26}x^3 + \frac{1}{26}x^4, \quad (8)$$

$$\Omega_{LDPC1}(x) = x^{19}, \quad (9)$$

$$\begin{aligned} \Lambda_{EP1}(x) = {} & \frac{2}{26}x^2 + \frac{2}{26}x^3 + \frac{4}{26}x^4 + \frac{3}{26}x^5 + \frac{1}{26}x^6 \\ & + \frac{4}{26}x^7 + \frac{4}{26}x^8 + \frac{3}{26}x^9 + \frac{1}{26}x^{10} \\ & + \frac{1}{26}x^{24} + \frac{1}{26}x^{27}, \end{aligned} \quad (10)$$

and

$$\begin{aligned} \Omega_{EP1}(x) = {} & \frac{1}{42}x^2 + \frac{5}{42}x^3 + \frac{18}{42}x^4 + \frac{8}{42}x^5 + \frac{5}{42}x^6 \\ & + \frac{2}{42}x^7 + \frac{2}{42}x^8 + \frac{1}{42}x^9. \end{aligned} \quad (11)$$

With $\Lambda_{LDPC1}(x)$, $\Omega_{LDPC1}(x)$, $\Lambda_{EP1}(x)$, $\Omega_{EP1}(x)$ is BG-1 degree distribution for VND of LDPC codes, CND of LDPC codes, VND of EP, and CND of EP, respectively. We do the similar procedure to obtain the EXIT chart of BG-2 as shown in Fig.3 with full EP. The degree distributions of BG-2 is

$$\Lambda_{LDPC2}(x) = \frac{6}{14}x^2 + \frac{8}{14}x^3, \quad (12)$$

$$\Omega_{LDPC2}(x) = \frac{2}{4}x^8 + \frac{2}{4}x^1 0, \quad (13)$$

$$\begin{aligned} \Lambda 1_{EP2}(x) = {} & \frac{2}{14}x^2 + \frac{1}{14}x^3 + \frac{1}{14}x^4 + \frac{1}{14}x^5 + \frac{2}{14}x^6 \\ & + \frac{1}{14}x^8 + \frac{1}{14}x^{10} + \frac{1}{14}x^{11} + \frac{1}{14}x^{12} \\ & + \frac{1}{14}x^{14} + \frac{1}{14}x^{19} + \frac{1}{14}x^{20}, \end{aligned} \quad (14)$$

and

$$\Omega_{EP2}(x) = \frac{6}{38}x^2 + \frac{20}{38}x^3 + \frac{9}{38}x^4 + \frac{3}{38}x^5. \quad (15)$$

With $\Lambda_{LDPC2}(x)$, $\Omega_{LDPC2}(x)$, $\Lambda_{EP2}(x)$, $\Omega_{EP2}(x)$ is BG-2 degree distribution for VND of LDPC codes, CND of LDPC codes, VND of EP, and CND of EP, respectively.

IV. EXIT Analysis of QC-LDPC Codes for Incremental Redundancy

We evaluate EXIT chart of 5G NR QC-LDPC codes based on BG-1 and BG-2 with full EP to observe the maximum benefit of EP. In this paper, we consider lifting size $Z = 64$ for 5G NR QC-LDPC codes BG-1 and BG-2.

Fig. 2 and Fig. 3 show EXIT charts of 5G NR QC-LDPC codes based on BG-1 and BG-2 with full EP, where the tunnel open until (1.0, 1.0) point without intersection point. EXIT curves are validated by EXIT trajectory at $E_b/N_0 = 0.3$ dB and $E_b/N_0 = 0$ dB, where the EXIT trajectory with iteration pattern $\mathcal{G} = 10(\mathcal{L} = 1, \mathcal{I} = 10)$ is confirming the validity of the curves.

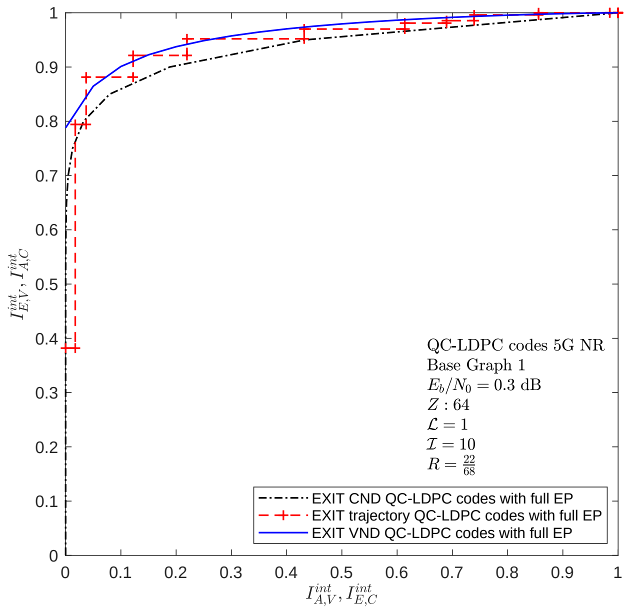

Fig. 2: EXIT chart of QC-LDPC codes based on BG-1 with full EP.

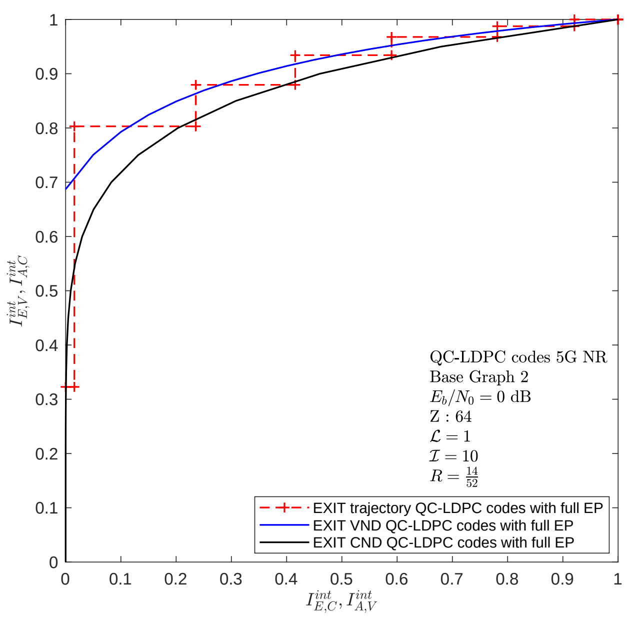

Fig. 3: EXIT chart of QC-LDPC codes based on BG-2 with full EP.

Since the tunnel of EXIT chart of BG-2 opens at $E_b/N_0 = 0$ dB, we can conclude that the performance of BG-2 is better than BG-1, where tunnel opens at $E_b/N_0 = 0.3$ dB.

V. Conclusion

We have analysed the EXIT chart of 5G NR QC-LDPC codes based on BG-1 and BG-2. We found that 5G NR based on BG-2 have better performances compared to BG-1 as a consequence of lower coding rates. It indicates that BG-2 is compatible for high reliability applications. On the other hand, BG-1 is more suitable for high data rate applications.

References

[1] S. V. S. Ranganathan, D. Divsalar, and R. D. Wesel, “Design of improved quasi-cyclic protograph-based Raptor-like LDPC codes for short block-lengths,” in *2017 IEEE International Symposium on Information Theory (ISIT)*, June 2017, pp. 1207–1211.

[2] T. M. Cover and J. A. Thomas, *Elements of Information Theory*, 2nd ed. Wiley, 2006.

[3] S. H. Kim and B. C. Jung, “On the optimal link adaptation in linear relay networks with incremental redundancy HARQ,” *IEEE Communications Letters*, vol. 18, no. 8, pp. 1411–1414, Aug., 2014.

[4] Y. Julian, R. Pudjiastuti, and K. Anwar, “Exit analysis for decoding behaviour and performances of 5G NR QC-LDPC codes,” in *The 21st International Symposium On Wireless Personal Multimedia Communications*, Nov. 2018.

[5] 3GPP, “New radio; multiplexing and channel coding,” *Tech. Rep.*, 2017.

[6] S. ten Brink, “Convergence behavior of iteratively decoded parallel concatenated codes,” *IEEE Trans. Commun.*, vol. 49, pp. 1727–1737, Oct. 2001.